Cellular Physiology and Biochemistry

Cell Physiol Biochem 2020;54:959-974
DOI: 10.33594/000000281
Published online: 1 October 2020
Accepted: 7 July 2020

Original Paper

Indole-6-Carboxaldehyde Isolated from *Sargassum thunbergii* (Mertens) Kuntze Prevents Oxidative Stress-Induced Cellular Damage in V79-4 Chinese Hamster Lung Fibroblasts through the Activation of the Nrf2/HO-1 Signaling Pathway

Sung Ok Kim[a] Yung Hyun Choi[b,c]

[a]Department of Food Science and Biotechnology, College of Engineering, Kyungsung University, Busan, Republic of Korea, [b]Anti-Aging Research Center, Dong-eui University, Busan, Republic of Korea, [c]Department of Biochemistry, Dong-eui University College of Korean Medicine, Busan, Republic of Korea

Key Words
I6CA • ROS • DNA damage • Apoptosis • Nrf2/HO-1

Abstract
Background/Aims: The disruption of redox equilibrium by oxidative stress, which is characterized by an overproduction of reactive oxygen species (ROS), is considered to be associated with fibroblast death in severe lung diseases. Indole-6-carboxaldehyde (I6CA) is a natural indole derivative isolated from *Sargassum thunbergii*, which a type of brown algae. However, the antioxidative effects of I6CA, and their mechanisms, have not been identified. This study was conducted to investigate the potential protective effects of I6CA against oxidative stress in V79-4 Chinese hamster lung fibroblasts. ***Methods:*** Cell viability and mechanisms related to antioxidant activity of I6CA (ROS production, cell cycle, DNA damage, mitochondrial membrane potential (MMP) and apoptosis) were studied. Western blot analysis was carried out to understand the involvement of various genes at protein level. ***Results:*** Our results demonstrated that I6CA inhibited hydrogen peroxide (H_2O_2)-induced cytotoxicity by blocking abnormal ROS accumulation. H_2O_2 treatment of V79-4 fibroblasts caused cell cycle arrest at the G2/M phase, which was accompanied by increased expression of the cyclin-dependent kinase (Cdk) inhibitor $p21^{WAF1/CIP1}$ and decreased expression of cyclin B1 and cyclin A. However, these effects were attenuated by treatment with I6CA. I6CA also effectively protected V79-4 cells against H_2O_2-induced apoptosis by increasing the Bcl-2/Bax ratio and suppressing the loss of MMP and the cytosolic release of cytochrome *c*. In addition, the activation of nuclear

Sung Ok Kim
and Yung Hyun Choi

Department of Food Science and Biotechnology, College of Engineering, Kyungsung University, 309, Suyeong-ro, Busan 48434 (Republic of Korea)
Tel. +82-51-663-4655, E-Mail theresa10000@naver.com

Department of Biochemistry, Dong-eui University College of Korean Medicine, 52-57, Yangjeong-ro, Busan 47227, Republic of Korea
Tel. +82-51-890-3319, Fax +82-51-890-3333, E-Mail choiyh@deu.ac.kr

factor-erythroid-2-related factor 2 (Nrf2) was markedly promoted by I6CA, which was associated with enhanced expression and activity of heme oxygenase-1 (HO-1). However, inhibiting the activity of HO-1 by zinc protoporphyrin IX, a potent inhibitor of HO-1, eliminated the ROS scavenging and anti-apoptotic effects of I6CA, indicating that I6CA was able to protect V79-4 lung fibroblasts from H_2O_2-induced oxidative stress by activating the Nrf2 signaling pathway. ***Conclusion:*** We suggest that I6CA may be useful as a candidate therapeutic agent for the treatment of oxidative stress-related lung diseases.

Introduction

The imbalance between the oxidant and antioxidant systems is an important step in the onset and progression of disease in most organs, including the lungs [1, 2]. Aerobic organisms, including humans, use oxygen as an electron acceptor during oxidative phosphorylation in mitochondria, and this process may be the largest source of free oxygen radicals, such as reactive oxygen species (ROS) [3, 4]. Under physiological conditions, ROS act as appropriate intracellular signaling molecules, but excessive accumulation of ROS during constant exposure to oxidative stress results in oxidative modification to nucleic acids, proteins, lipids and other small intracellular molecules [5, 6]. Furthermore, there is increasing evidence that high levels of ROS and other oxygen-induced free radicals due to the imbalance of the redox equilibrium can contribute to inhibition of proliferation and induction of apoptosis in lung fibroblasts [7, 8]. Therefore, research on new antioxidants and their mechanisms has been recognized as a strategy for the prevention and treatment of oxidative stress-mediated lung diseases.

Indole and its derivative compounds, which have an aromatic heterocyclic structure, are biologically active molecules formed from naturally occurring glucosinolates. These compounds are found not only in cruciferous vegetables but also in a number of natural resources, including actinomycetes, fungi, algae and marine sponges [9, 10]. Many studies have shown that indole derivatives have received considerable attention due to their potential health-enhancing properties, including antiviral [11, 12], antibacterial [13, 14], anti-inflammatory [14-16], antioxidant [14, 17-19], and anti-cancer activities [20, 21] as well as their inhibitory effects against various cardiovascular and metabolic diseases [22-24]. In particular, many studies have shown that indole derivatives can activate antioxidant defense systems and improve damage against oxidative stress. For example, the activation of nuclear factor-erythroid 2-related factor 2 (Nrf2), one of the most important transcription factors that regulates the production of antioxidant enzymes that protect against oxidative stress, plays a key role in the antioxidant efficacy of some indole derivatives in various *in vitro* and *in vivo* models [25-30]. Some investigations have shown that the Nrf2-mediated increased expression of heme oxygenase-1 (HO-1), which is induced some of these indole derivatives, contributes to the inhibition of DNA damage and/or apoptosis caused by oxidative stress [28-30].

Recently, in the process of exploring novel indole derivatives with anti-obesity effects, Kang et al. [31] found that indole-6-carboxaldehyde (I6CA) isolated from the marine brown algae *Sargassum thunbergii* (Mertens) Kuntze is an effective candidate. In addition, Kim et al. [32] reported that this derivative suppressed tumor invasion and metastasis by inhibiting the activity of matrix metalloproteinase-9 and preventing degradation of the extracellular matrix. However, to date, there is a lack of evidence to describe the underlying mechanisms and limited information available about whether I6CA can reduce oxidative stress-induced damage. Therefore, in this study, we evaluated the beneficial effect of I6CA against oxidative stress (H_2O_2)-induced cytotoxicity in V79-4 Chinese hamster lung fibroblasts. In addition, the relevance of the Nrf2 signaling pathway was investigated to determine whether this pathway is involved in the I6CA-mediated antioxidant mechanism.

Materials and Methods

Reagents and antibodies

Dulbecco's modified Eagle's medium (DMEM), fetal calf serum (FCS), antibiotics mixtures, and other cell culture reagents were obtained from WelGENE Inc. (Gyeongsan, Republic of Korea). I6CA, H_2O_2, N-acetyl-L-cysteine (NAC), zinc protoporphyrin IX (ZnPP), 3-(4,5-dimethylthiazol-2-yl)-2,5-diphenyltetra-zolium bromide (MTT), propidium iodide (PI), DNase-free RNase A, 4,6-diamidino-2-phenylindole (DAPI) and 5,5',6,6'-tetrachloro-1,1'3,3'-tetraethyl-imidacarbocyanune iodide (JC-1), were purchased from Sigma-Aldrich Chemical Co. (St. Louis, MO, USA). 2',7'-Dichlorofluorescein diacetate (DCF-DA) and annexin V-fluorescein isothiocyanate (FITC) apoptosis detection kit were purchased from Molecular Probes (Eugene, OR, USA) and R&D Systems Inc. (Minneapolis, MN, USA), respectively. The mitochondria and cytoplasmic protein extraction kit and Bradford assay reagent were obtained from Active Motif, Inc. (Carlsbad, CA, USA) and Bio-Rad Laboratories (Hercules, CA, USA), respectively. Polyvinylidene difluoride (PVDF) membranes were purchased from Merck Millipore (Bedford, MA, USA). Genomic DNA purification kit and HT 8-oxo-dG enzyme-linked immunosorbent assay (ELISA) kit were supplied by Promega Corporation (*Madison*, WI, USA) and Trevigen (Gaithersburg, MD, USA), respectively. Primary antibodies were purchased from Abcam, Inc. (Cambridge, MA, UK), Cell Signaling Technology (Danvers, MA, USA), and Santa Cruz Biotechnology, Inc. Horseradish peroxidase (HRP)-conjugated secondary antibodies and enhanced chemiluminescence (ECL) detection system were obtained from Amersham Life Science (Arlington Heights, IL, USA). HO-1 ELISA kit was purchased from Abcam, Inc. All other chemicals not specifically cited here were supplied by Sigma-Aldrich Chemical Co.

Cell culture and I6CA treatment

Chinese hamster lung fibroblast V79-4 cell line was obtained from the American Type Culture Collection (Manassas, VA, USA) and cultured in DMEM supplemented with 10% heat-inactivated FCS and antibiotics mixture in a humid atmosphere of 95% air and 5% CO_2 and 37°C. Cells in the logarithmic growth phase were used in subsequent experimentation. I6CA was dissolved in dimethyl sulfoxide (DMSO), and diluted with cell culture medium to adjust the final treatment concentrations before use in experiments.

Cell viability assay

Cell viability was measured using an MTT assay as described by Kim et al. [33]. V79-4 cells were seeded into 96-well plates in culture medium overnight, and then treated with various concentrations of I6CA or H_2O_2 for 24 h or pretreated with I6CA, NAC or ZnPP for 1 h and then incubated with or without H_2O_2 for 24 h. Then, MTT solution was then added to a final concentration of 0.5 mg/ml and incubated at 37°C for 3 h. At the end of the incubation, the culture supernatants were carefully discarded, and the formed formazan crystals were dissolved in DMSO. Finally, the optical density values were acquired with an ELISA reader (Dynatech Laboratories, Chantilly, VA, USA) at 450 nm. The optical density of the formazan crystals formed in untreated control cells was used to represent 100% viability. In a parallel experiment, changes in cell images were captured by a phase-contrast microscope (Carl Zeiss, Oberkochen, Germany).

Measurement of ROS generation

To measure the amount of ROS generated in cells, cells were treated with or without I6CA or NAC for 1 h before another 1 h culture in the presence of H_2O_2. The cells were washed with phosphate-buffered saline (PBS), and lysed with PBS containing 1% Triton X-100 for 10 min at 37°C. The cells were stained with 10 μM DCF-DA for 30 min in the dark. Intracellular ROS production was immediately recorded at 515 nm by a flow cytometer (Becton Dickinson, San Jose, CA, USA) [34]. The results were expressed as the percentage increase relative to untreated cells. It was also analyzed the levels in ROS by fluorescence microscopy. To this end, cells cultured in glass cover slips were treated with H_2O_2 in the absence or presence of I6CA or NAC. After 1 h of treatment, the cells were fixed in 4% polyformaldehyde for 30 min at 4℃ and incubated in a medium containing 10 μM DCF-DA at 37°C for 20 min. Stained cells were washed twice with PBS and observed with a fluorescence microscope (Carl Zeiss).

Cell cycle analysis

To analyze cell cycle distribution using PI staining, the cells were treated with or without I6CA or NAC for 1 h before being cultured with H_2O_2 for 24 h. The cells were washed twice with PBS, resuspended gently in 70% ethanol and fixed at 4°C overnight. The cells were washed with PBS and incubated with 0.1 mg/ml DNase-free RNase A at 37°C for 1 h and stained with 40 μg/ml PI at 37°C for 30 min before flow cytometric analysis. The samples were analyzed using a flow cytometer at 488/575 nm excitation/emission, and the proportion of cells in the sub-G1, G1, S, and G2 phases was measured using CellQuest software (Becton Dickinson) and Modfit LT 3.0 software (Verity Software House Inc., Topsham, ME, USA).

Western blot analysis

At the end of the treatment period, the cells were collected and lysed on ice for 30 min in lysis buffer as previously described [34]. The mitochondrial and cytoplasmic protein fractions were obtained using a commercial mitochondrial fractionation kit according to the manufacturer's instructions. The protein concentration of the collected supernatants was measured using the Bradford assay reagent according to the manufacturer's protocol. Subsequently, equal amounts of protein from each sample was separated by sodium-dodecyl sulfate (SDS)-polyacrylamide gel electrophoresis and transferred to PVDF membranes. The membranes were blocked with Tris-buffered saline (10 mM Tris-Cl, pH 7.4) containing 5% skim milk and 0.5% Tween-20 for 1 h at room temperature (RT) and then incubated overnight at 4°C with primary antibodies. After washing with PBS, the membranes were incubated with the appropriate HRP-conjugated secondary antibodies for 2 h at RT. The protein bands were detected using an ECL detection system, and the signals were visualized using a chemiluminescence imager (Azure Biosystems, Inc., Dublin, CA, USA).

Nuclear staining

To determine apoptosis, changes in nuclear morphology were examined using DAPI staining. Briefly, cells were harvested after treatment with H_2O_2 in the absence or presence of I6CA or NAC, washed with PBS, and fixed with 4% paraformaldehyde in PBS for 10 min at RT. The cells were washed with PBS again and stained with 2.5 μg/ml DAPI solution for 10 min at RT. The cells were observed *via* a fluorescence microscope.

Comet assay

A comet assay was used to analyze the migration of the DNA from individual cells in the gel as previously described [35]. After the cells were exposed to H_2O_2 with or without I6CA or NAC, the cells were suspended in 0.5% low melting point agarose (LMA) at 37°C, aliquoted and then spread onto a fully frosted microscope slide precoated with 1% normal melting agarose. After the agarose solidified in the dark, the slide was covered with 0.5% LMA and submerged in lysis solution for 1 h at 4°C. The slides were then incubated in a gel electrophoresis device containing 300 mM NaOH and 10 mM Na-EDTA (pH 13) for 30 min and then were subjected to electrophoresis for 30 min at 300 mA for 20 min to draw negatively charged DNA toward the anode. When electrophoresis was complete, the slides were washed with neutralizing buffer at 4°C and stained with 20 μg/mL PI. The nuclear images were visualized and captured using a fluorescence microscope.

Determination of 8-hydroxy-2'-deoxyguanosine (8-OHdG) concentration

After experimental treatment, the levels of intracellular 8-OHdG, a ubiquitous marker of DNA damage due to oxidative stress, were quantitated using the HT 8-oxo-dG ELISA Kit, according to the manufacturer's protocol. Briefly, after treatment with H_2O_2 in the absence or presence of I6CA, the cells were trypsinized. DNA was extracted using the Genomic DNA purification kit and was quantitated, and the DNA concentration of each sample was adjusted to a final concentration of 200 μg/ml. Then, the DNA was digested by DNase I and alkaline phosphatase sequentially for 1 h at 37°C. To determine the levels of 8-OHdG in the culture supernatants, the cell culture medium was clarified by centrifugation of the cell debris, and the amount of 8-OHdG was measured at 450 nm using an ELISA plate reader based on the manufacturer's instructions. Subsequently, the concentration of 8-OHdG for each sample was quantified from the standard curve.

HO-1 activity assay

The HO-1 enzyme activity was estimated by measuring the rate of conversion to bilirubin in heme using a HO-1 ELISA kit. In brief, the cells were lysed with the extraction reagent included in the kit in accordance with the manufacturer's instructions. After quantifying the protein concentration, the cell lysates were incubated with the reaction mixtures at 23°C for 30 min, whereas the blank samples were incubated with hemin alone. The amount of bilirubin formed was calculated according to the difference in the absorbance between the 464 and 530 nm wavelengths using an ELISA reader. The HO-1 activity was determined as picomoles of bilirubin per milligram of protein based on the standard bilirubin curve.

Measurement of mitochondrial membrane potential (MMP, $\Delta\psi_m$)

Mitochondrial function was determined by membrane potential-specific fluorescence staining using a sensor of mitochondrial potential, JC-1. In brief, the collected cell pellets were suspended in PBS and incubated with 10 μM JC-1 at 37°C for 20 min. The cells were then washed with cold PBS and analyzed using a flow cytometer. We also analyzed the changes in the MMP by fluorescence microscopy. To this end, the cells cultured on glass cover slips were treated with H_2O_2 in the absence or presence of I6CA. After 24 h of treatment, the cells were incubated in a medium containing 10 μM JC-1 at 37°C for 20 min. The stained cells were washed twice with PBS and observed with a fluorescence microscope.

Detection of apoptosis by annexin V staining

The degree of apoptosis was detected using an annexin V-FITC apoptosis detection kit according to the manufacturer's instructions. In brief, after treatment with H_2O_2 in the absence or presence of I6CA or ZnPP, the collected cells were washed with cold PBS, fixed in 75% ethanol at 4°C for 30 min and then stained with annexin V-FITC and PI for 20 min at RT in the dark. Using a flow cytometer, the fluorescence intensities of the cells were quantified as percentages of annexin V-positive and PI-negative (annexin V^+/PI^-) cells in the total cell populations as indicators of apoptotic cells, whereas the V^-/PI^- cells in the total cell population was considered normal [36].

Statistical analysis

Results are expressed as the mean ± standard deviation (SD) of at least three independent experiments. Statistical analyses were performed using the SPSS software, version 16.0 (SPSS Inc., Chicago, IL, USA). Significance was analyzed by one-way ANOVA. A value of $p<0.05$ was considered to indicate a significant difference.

Results

I6CA suppresses the H_2O_2-induced reduction in cell viability in V79-4 cells

Fig. 1A shows that in the cells treated with I6CA at concentrations below 300 μM, there was no significant difference in the cell viability compared to the control, but treatment with I6CA at concentration over 400 μg/ml slightly decreased the viability of the V79-4 cells. Therefore, to study the cytoprotective effects of I6CA against H_2O_2-induced oxidative stress, a 300 μM concentration of I6CA was chosen. Next, to achieve the optimized oxidative stress conditions, the cells were treated with different concentrations of H_2O_2 for 24 h. As shown in Fig. 1B, the viability of V79-4 cells exposed to H_2O_2 was significantly reduced in a concentration-dependent manner, and the 1 mM concentration of H_2O_2, which led to a survival rate of approximately 60%, was selected for the induction of cytotoxicity in the subsequent experiments. To assess the cytoprotective effect of I6CA, the cells were pretreated with 300 μM I6CA for 1 h, followed by 1 mM $H_2O_2$for 24 h, and it was found that I6CA significantly inhibited the H_2O_2-mediated reduction in V79-4 cell viability (Fig. 1C). We also found that pretreatment with NAC, a well-established ROS scavenger, completely inhibited H_2O_2-induced cytotoxicity when compared with the controls (Fig. 1C). In addition, the morphological changes in the V79-4 cells treated with H_2O_2 alone were alleviated by pretreatment with I6CA or NAC (Fig. 1D).

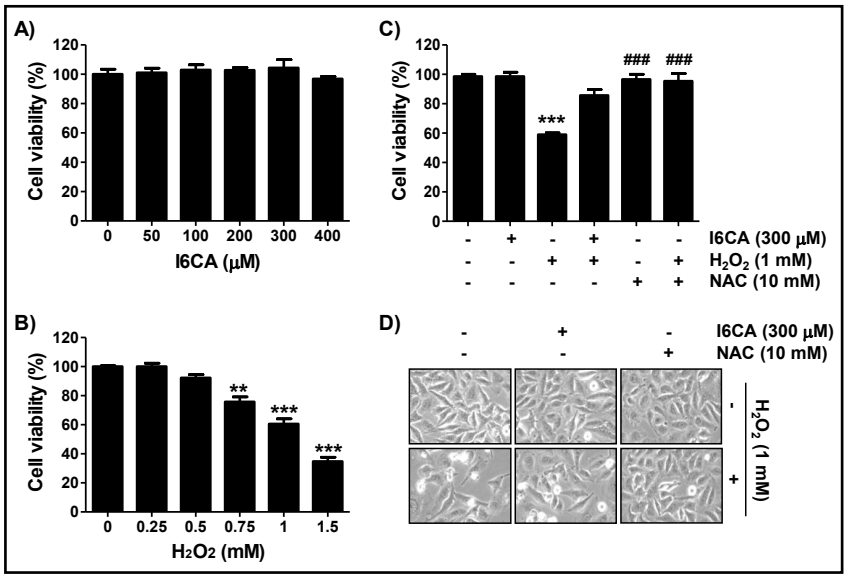

Fig. 1. Protective effect of I6CA on H_2O_2-induced cytotoxicity in V79-4 cells. The cells were treated with various concentrations of I6CA (A) or H_2O_2 (B) for 24 h or pretreated with or without 300 μM I6CA or 10 mM NAC for 1 h and then cultured in the presence of 1 mM H_2O_2 for 24 h (C and D). (A-C) The cell viability was determined by an MTT assay. The results are expressed as the mean ± SD obtained from three independent experiments (**p<0.01 and ***p<0.001 compared with the control group; ###p<0.001 compared with the H_2O_2-treated group). (D) Representative images of the cells were captured by a phase-contrast microscope (original magnification, 200×).

I6CA reverses H_2O_2-induced ROS generation in V79-4 cells

We next investigated whether I6CA eliminated H_2O_2-induced ROS accumulation using a fluorescent indicator, DCF-DA, and found that the accumulation of ROS in H_2O_2-treated V79-4 cells peaked within 1 h and gradually decreased over time (data not shown). However, pretreatment with I6CA significantly reduced the effect of H_2O_2 on ROS overproduction, and NAC also almost completely eliminated the accumulation of ROS (Fig. 2A and B). Similarly, I6CA protected H_2O_2-induced DCF fluorescence in the cells (Fig. 2C).

I6CA inhibits H_2O_2-induced G2/M arrest in V79-4 cells

As shown in the flow cytometry results in Fig. 3A, the inhibition of V79-4 cell viability following H_2O_2 treatment was associated with cell cycle arrest at the G2/M phase. In addition, the percentage of cells in the sub-G1 phase H_2O_2-treated V79-4 cells, which was used as an index of apoptotic cells, increased, whereas the ratio of the cells in the G1 and S phases decreased (Fig. 3A and B). The immunoblotting results revealed that the expression of the cyclin-dependent kinase (Cdk) inhibitor $p21^{WAF1/CIP1}$ significantly increased, and the expression of cyclin A and cyclin B1 decreased (Fig. 3B). However, pretreatment with I6CA significantly attenuated the H_2O_2-induced G2/M arrest, which was associated with a decreased percentage of cells in the sub-G1 phase. In parallel, the increased $p21^{WAF1/CIP1}$ expression induced by H_2O_2 was greatly reduced in the presence of I6CA, whereas the reduced expression of cyclin A and cyclin B1 was restored (Fig. 3C). Even under the conditions that artificially blocked the production of ROS using NAC, these changes were dramatically diminished. Moreover, V79-4 cells exposed to H_2O_2 alone demonstrated characteristic apoptotic features, including nuclear condensation and fragmentation, and pretreatment with I6CA or NAC markedly reduced these morphological changes (Fig. 3D).

I6CA attenuates H_2O_2-induced DNA damage in V79-4 cells

To investigate whether I6CA can prevent DNA damage by H_2O_2, we performed an alkaline comet assay. As shown in the representative images in Fig. 4A, no apparent comet tail moment (DNA migration) was observed in the cells treated with I6CA alone or the control cells, whereas markedly increased DNA migration was observed in the H_2O_2-treated cells.

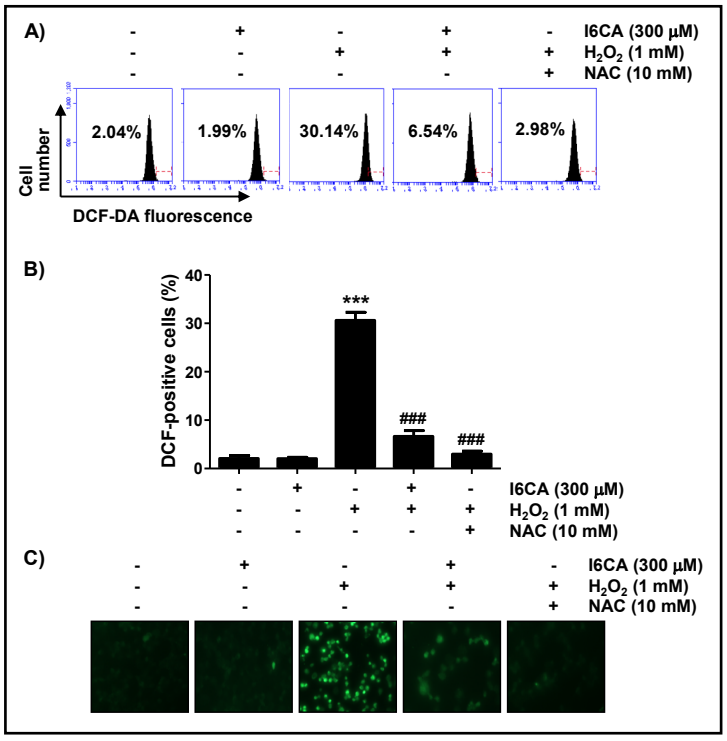

Fig. 2. Attenuation of H_2O_2-induced ROS generation by I6CA in V79-4 cells. The cells were pretreated with 300 μM I6CA or 10 mM NAC for 1 h and then stimulated with or without 1 mM H_2O_2 for an additional 1 h. The medium was removed, and the cells were incubated with medium containing DCF-DA for 30 min. (A) ROS production was measured using a flow cytometer, and representative profiles are shown. (B) The measurements were made in triplicate, and the values are expressed as the mean ± SD (***p<0.001 compared with the control group; ###p<0.001 compared with the H_2O_2-treated group). (C) DCF fluorescence images of cells cultured under the same conditions were captured by a phase-contrast microscope (original magnification, 200×). Each image is representative of at least three independent experiments.

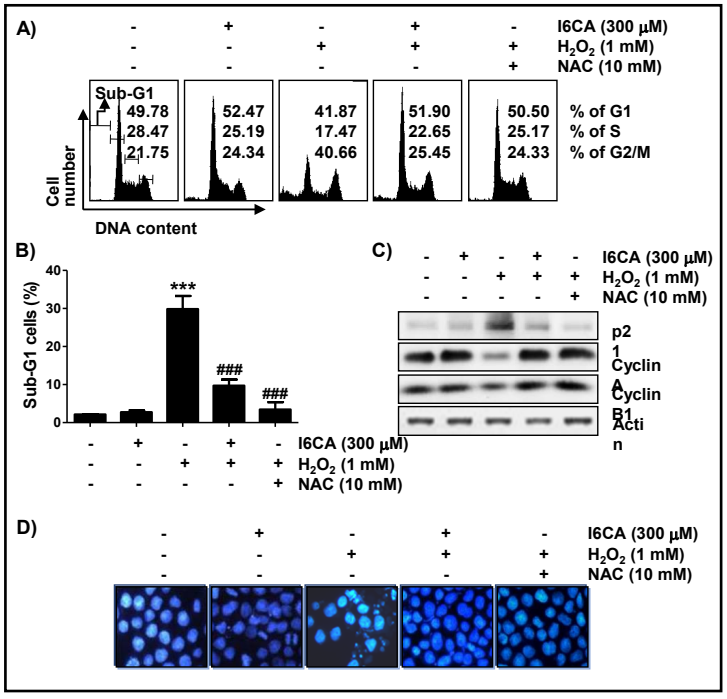

Fig. 3. Inhibitory effect of I6CA on H2O2-induced cell cycle arrest in V79-4 cells. The cells were pretreated with or without 300 μM I6CA or 10 mM NAC for 1 h before treatment with 1 mM H2O2 for 24 h. (A) The cells were stained with PI solution for flow cytometry analysis. The average percentages of cells in each phase of the cell cycle, except for the cells in the sub-G1 phase, are displayed. (B) Sub-G1% was calculated as the number of cells in the sub-G1 phase relative to the number of total cells. The results are expressed as the mean ± SD obtained from three independent experiments (***p<0.001 compared with the control group; ###p<0.001 compared with the H2O2-treated group). (C) Total cell lysates were prepared, and equal amounts of proteins were subjected to Western blot analysis of the listed proteins. Actin was used as an internal control, and the proteins were visualized using an ECL detection system. (D) The cells were stained with DAPI solution, and the stained nuclei were observed using a fluorescence microscope (original magnification, 200×). Each image is representative of at least three independent experiments.

However, pretreatment with I6CA or NAC clearly reduced the H_2O_2-induced the DNA migration to levels similar to those observed in the control cells. The DNA damage blocking effect of I6CA was also confirmed by analyzing the phosphorylation of γH2AX (p-γH2AX) and the production of 8-OHdG. As shown in Fig. 4B and C, although no significant change was observed in the total protein expression of γH2AX in the cells treated with H_2O_2 alone, the expression of p-γH2AX obviously increased, and higher levels of 8-OHdG were also observed in the H_2O_2-treated cells. However, pretreatment with I6CA or NAC clearly attenuated the H_2O_2-induced phosphorylation of γH2AX and significantly suppressed the production of 8-OhdG.

I6CA reduces H_2O_2-induced mitochondrial dysfunction in V79-4 cells

To analyze whether inhibition of mitochondrial impairment is a mechanism involved in the cytoprotective effect of I6CA, JC-1 dye was used to estimate the MMP. As shown in Fig. 5A and B, a significant decrease in the ratio of JC-1 monomers and an increase in JC-1 aggregates were observed in the cells exposed to H_2O_2. The ratio of red/green fluorescence was also significantly decreased after H_2O_2 treatment compared with untreated group (Fig. 5C), indicating that H_2O_2 reduced the MMP. In addition, the expression of cytochrome *c* in the H_2O_2-treated cells increased in the cytoplasmic fraction and decreased in the mitochondrial fraction (Fig. 5D), indicating that cytochrome *c* was released from the mitochondria to the cytosol. The expression of the anti-apoptotic Bcl-2 protein decreased and that of the pro-apoptotic protein Bax increased, and degradation of the poly (ADP-ribose) polymerase (PARP) protein was also observed in the H_2O_2-treated cells (Fig. 6E). However, pretreatment with I6CA reversed these changes.

I6CA activates the Nrf2/HO-1 signaling pathway in V79-4 cells

We further investigated whether the antioxidant activity of I6CA was correlated with the activation of the Nrf2/HO-1 signaling pathway. The immunoblotting results indicated that the expression of Nrf2 and its phosphorylation (p-Nrf2) were slightly increased in the cells treated with H_2O_2 alone compared with untreated control, but their expression greatly increased in the cells cotreated with H_2O_2 and I6CA (Fig. 6A). In addition, the expression

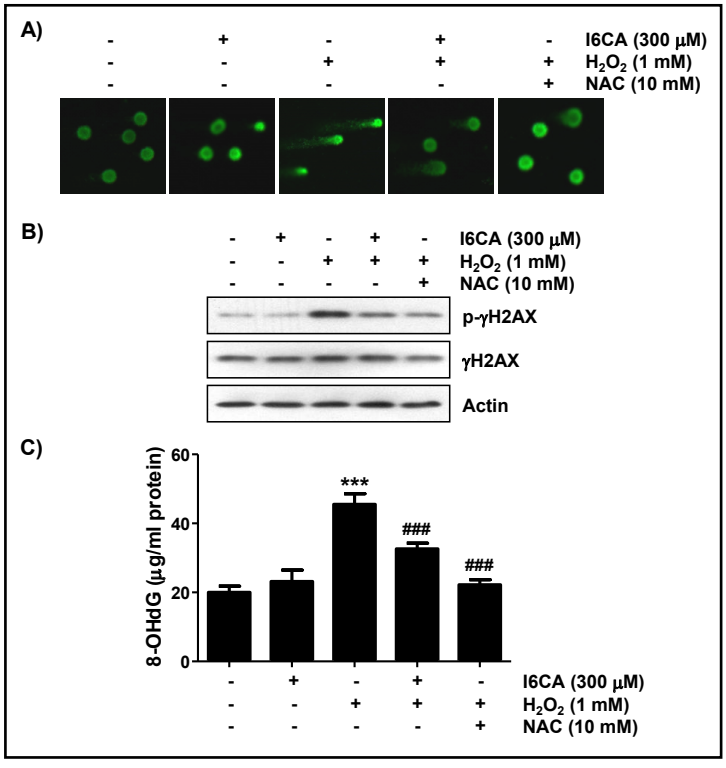

Fig. 4. Protection of H_2O_2-induced DNA damage by I6CA in V79-4 cells. The **c**ells were treated with or without 300 μM I6CA or 10 mM NAC for 1 h before treatment with 1 mM H_2O_2 for 24 h. (A) A comet assay was performed, and representative images were captured using a fluorescence microscope (original magnification, ×200). (B) The cell lysates were prepared, and p-γH2AX and γH2AX expression was identified by Western blot analysis. The equivalent loading of proteins in each well was confirmed by actin. (C) The DNA samples of cells were subjected to assessment of the 8-OHdG levels. The measurements were made in triplicate, and the results are expressed as the mean ± SD (***p<0.001 compared with the control group; ###p<0.001 compared with the H_2O_2-treated group).

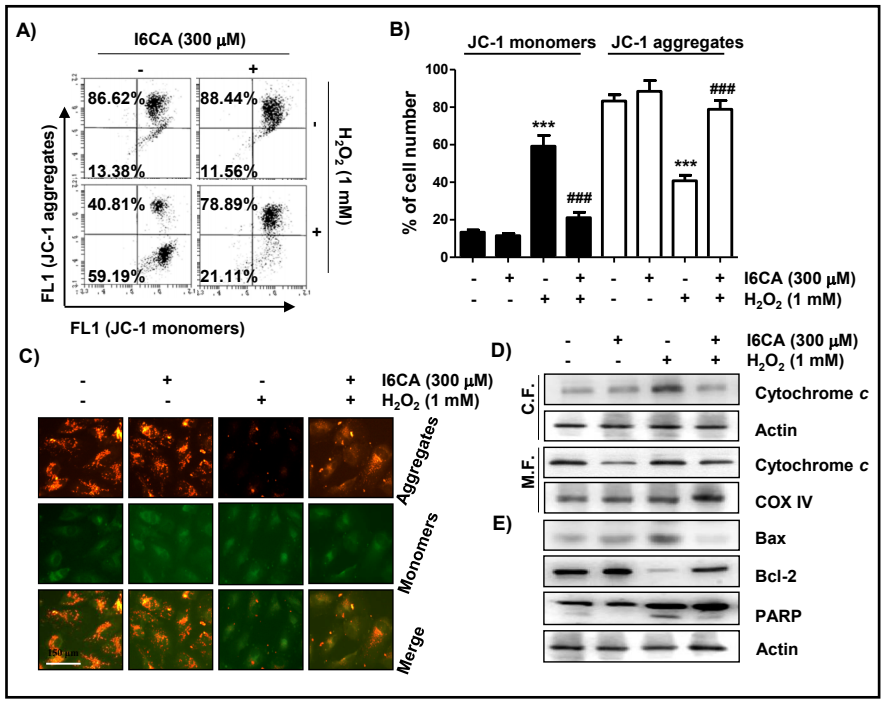

Fig. 5. Inhibition of H_2O_2-induced mitochondrial dysfunction by I6CA in V79-4 cells. The cells were treated with 300 μM I6CA for 1 h and then exposed to 1 mM H_2O_2 for 24 h. (A) The cells were collected and stained with JC-1. The JC-1 fluorescence intensity was detected to evaluate the changes in the MMP using a flow cytometer. (B) The percentages of cells with JC-1 monomers and aggregates are indicated by bars, and the data represent the mean ± SD of triplicate determinations (***p<0.001 compared with the control group; ###p<0.001 compared with the H_2O_2-treated group). (C) JC-1 fluorescence images of the cells treated with 1 mM H_2O_2 in the presence or absence of 300 μM I6CA are shown. Red fluorescence indicates high membrane potential, and green fluorescence represents low membrane potential. (D) Western blot analysis of cytochrome *c* levels in the mitochondrial and cytosolic fractions isolated from the cells cultured under the same conditions. Cytochrome oxidase subunit VI (COX IV) and actin serve as protein loading controls for the mitochondria and cytosol, respectively. (E) Whole cell lysates were prepared, and Bax, Bcl-2 and PARP expression was identified by Western blot analysis. The equivalent loading of proteins in each well was confirmed by actin.

of the HO-1 protein was similarly upregulated, and the HO-1 activity was also significantly increased in the cells treated with both H_2O_2 and I6CA compared with the cells treated with H_2O_2 alone or control (Fig. 6A and B). In contrast, the expression of Kelch-like ECH-associated protein-1 (Keap1), a negative regulator of Nrf2, was relatively reduced in the cells treated with I6CA and H_2O_2.

Nrf2/HO-1 signaling pathway is involved in the mitigation of H_2O_2-mediated apoptosis by I6CA in V79-4 cells

Finally, we investigated whether the activation of the Nrf2/HO-1 signaling pathway was directly related to the antioxidant and anti-apoptotic effects of I6CA in V79-4 cells. As shown in Fig. 7A and B, when the HO-1 activity was blocked by ZnPP, a potent competitive inhibitor of HO-1, the inhibition of the intracellular ROS production by I6CA in H_2O_2-treated cells was reversed, indicating that I6CA exerted an antioxidant effect by activating Nrf2-mediated HO-1. In parallel, flow cytometry analysis using annexin V/PI staining showed that H_2O_2 triggered a higher degree of apoptosis compared with the control, whereas after pretreatment with I6CA, the percentage of apoptotic cells significantly decreased. However, the anti-apoptotic effect of I6CA in H_2O_2-stimulated cells was markedly reduced by treatment with ZnPP (Fig. 7C and D).

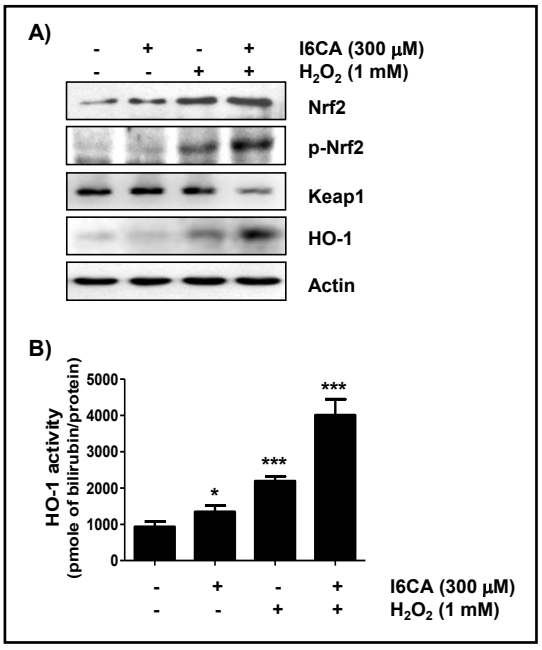

Fig. 6. Activation of the Nrf2/HO-1 signaling pathway by I6CA in V79-4 cells. (A) The cells were pretreated with 300 μM I6CA for 1 h and then treated with or without 1 mM H_2O_2 for 24 h. Equal amounts of proteins were separated by SDS-polyacrylamide gel electrophoresis and subjected to Western blot analysis of the listed proteins. Actin was used as an internal control. (B) The cells cultured under the same conditions as in (A) were lysed, and the HO-1 activity was calculated using a commercial kit according to the manufacturer's procedure. The measurements were made in triplicate, and the values are expressed as the mean ± SD (**p<0.05 and ***p<0.001 compared with the control group).

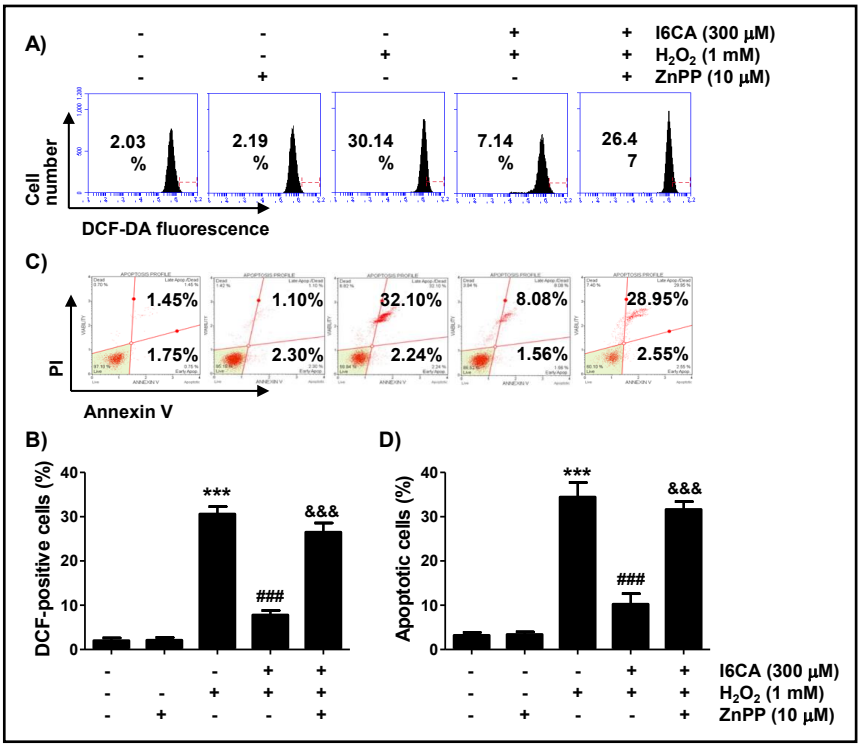

Fig. 7. Prevention of H_2O_2-induced apoptosis by I6CA was dependent on the activation of the Nrf2/HO-1 signaling pathway in V79-4 cells. The cells were treated with 300 μM I6CA or 10 μM ZnPP for 1 h and then treated with or without 1 mM H_2O_2 for an additional 1 h (A and B) or 24 h (C and D). (A) The medium was removed, and the cells were stained with DCF-DA. ROS production was measured using a flow cytometer, and representative profiles are shown. (C) The cells were stained with annexin V-FITC and PI for flow cytometry analysis, and representative profiles are presented. The percentages of apoptotic cells were determined by counting the percentages of annexin V-positive cells. (B and D) The data are expressed as the mean ± SD obtained from three independent experiments (***p<0.001 compared with the control group; ###p<0.001 compared with the H_2O_2-treated group; &&&p<0.001 compared with the I6CA and H_2O_2-treated group).

Discussion

As the discovery of novel indole derivatives from various natural sources increases, interest in their pharmacological efficacy is increasing. Among these indole derivatives, I6CA has been reported to inhibit adipogenesis and suppress cancer cell invasion and metastasis [31, 32], but information on its other pharmacological efficacies is still limited. Therefore, in this study, we investigated whether I6CA can protect V79-4 lung fibroblasts from oxidative stress. For this purpose, we utilized H_2O_2, which is widely used as a representative ROS for establishing various oxidative stress models, to induce oxidative damage, and we found that H_2O_2 reduced V79-4 cell viability by triggering G2/M cell cycle arrest, DNA damage and mitochondria-mediated apoptosis by promoting ROS production. However, I6CA has been found to have the ability to inhibit H_2O_2-induced cytotoxicity and provide ROS scavenging activity, and these functions are associated with the activation of the Nrf2/HO-1 signaling pathway.

Many previous studies have shown that the inhibition of cell proliferation and the induction of apoptosis by H_2O_2 are accompanied by the induction of G2/M cell cycle phase arrest in various *in vitro* models, including V79-4 lung fibroblasts [37-39]. Cell cycle progression during cell proliferation is achieved through the binding of cyclins with Cdks, which are essential for the progression of each phase, and their activities are inhibited by Cdk inhibitors [40, 41]. In agreement with a previous finding [38], the reduction of cell viability in H_2O_2-treated V79-4 cells was associated with G2/M phase arrest and apoptosis induction in this study. The upregulated expression of the Cdk inhibitor $p21^{WAF1/CIP1}$, a typical Cdk inhibitor belonging to the kinase inhibitory protein/Cdk interacting protein (KIP/CIP) family, and the downregulated expression of cyclin A and cyclin B1 were associated with the induction of G2/M arrest by H_2O_2, and these results are also consistent with the results of previous studies observed in various cell lines [42, 43]. During cell cycle progression, the transition from the G2 phase to the M phase requires increased Cdk2 and Cdk1 kinase activity by complexing cyclin A and B-type cyclins [41, 44]. However, Cdk inhibitors bind to Cdks, thereby inhibiting their activity and consequently disrupting cell cycle progression [40, 45]. In this study, increased p21 and decreased cyclin A and cyclin B1 expression levels by H_2O_2 were attenuated in the presence of I6CA, and G2/M arrest was also relieved. In addition, the DNA damage accompanying H_2O_2-induced apoptosis was also effectively reduced by I6CA. These phenomena were evident even when ROS production was blocked by NAC treatment. Although further research should be conducted to investigate other regulatory factors involved in the regulation of cell cycle progression and DNA damage, the current data showed that the ROS scavenging ability of I6CA contributed to reversing the V79-4 cell viability inhibition associated with the cell cycle arrest and DNA damage caused by H_2O_2.

Apoptosis, which is strictly regulated by various factors, can generally be divided into the extrinsic and intrinsic pathways. The former is initiated by extracellular ligands that bind to death receptors on the cell surface, and the latter is associated with intracellular apoptotic signals that cause mitochondrial dysfunction [46, 47]. Among the organelles in cells, mitochondria are most susceptible to excessive H_2O_2 insults, and their dysfunction greatly contributes to ROS production. ROS accumulation triggers free radical attack of the mitochondrial phospholipid bilayer, which leads to depolarization of the mitochondrial membrane, resulting in MMP loss [46, 48]. During this process, the permeability of the mitochondrial membranes increases, allowing apoptogenic factors in the mitochondrial intermembrane space, especially cytochrome *c*, to be released into the cytoplasm. Therefore, the loss of the MMP and the cytosolic release of cytochrome *c* are indicative of impaired mitochondrial function and are evident early phenomena in the onset of intrinsic apoptosis [47-49]. Therefore, to evaluate the preventive effect of I6CA on mitochondrial dysfunction, the MMP values and cytochrome *c* expression were examined, and it was found that the loss of the MMP and cytosolic cytochrome *c* expression was markedly increased in H_2O_2-treated V79-4 cells. However, I6CA pretreatment protected the reduction of the MMP induced by H_2O_2 and maintained the expression of cytochrome *c* in mitochondria during H_2O_2 exposure.

During the intrinsic apoptosis pathway, cytochrome *c* released into the cytoplasm interacts with and activates caspase-9, which in turn activates the downstream effector caspases to complete cell death. This process is accompanied by the degradation of the substrate proteins of the effector caspases, including PARP, as evidenced by caspase-dependent apoptosis [50, 51]. The activation of this caspase cascade is also tightly regulated by the expression of a variety of regulators. Among these regulators, the members of the Bcl-2 family, which is composed of pro-apoptotic and anti-apoptotic proteins, play an important role in determining the progression of the intrinsic apoptosis pathway. As a representative pro-apoptotic protein, Bax, located on the outer mitochondrial membrane, induces cytochrome *c* release by promoting mitochondrial permeability transition or weakening the barrier function of the mitochondrial outer membrane. Conversely, anti-apoptotic proteins, such as Bcl-2, are essential for maintaining mitochondrial permeability and membrane barrier stabilization to inhibit the release of apoptotic factors [47, 49]. Therefore, the balance between pro-apoptotic Bax member proteins and anti-apoptotic Bcl-2 member proteins acts as a determinant that induces the activation of the caspase cascade upon initiation of the intrinsic apoptotic pathway [50, 51]. In this study, the Bax/Bcl-2 expression ratio was improved in H_2O_2-treated V79-4 cells, and PARP degradation was increased. However, these changes were markedly reversed in the presence of I6CA, indicating that I6CA can protect V79-4 cells from apoptosis by inhibiting the intrinsic apoptosis pathway activated by oxidative stress. Collectively, the results of the present study demonstrated that the I6CA antagonism of apoptosis induced by H_2O_2 in V79-4 cells could occur through mitochondrial function repair.

Accumulating evidence has shown that Nrf2 is one of the major transcription factors that regulate the production of antioxidant enzymes to protect cells from oxidative stress. Under homeostatic conditions, Nrf2 binds to its negative regulator, Keap1, in the cytoplasm and constitutively degrades through the ubiquitin proteasome system. To promote the expression of antioxidant response element (ARE)-dependent antioxidant enzymes, phosphorylation of Nrf2 by the intracellular kinase signal transduction pathway is required for translocation to the nucleus after dissociation from Keap1 [52, 53]. HO-1, one of the key inducible phase II enzymes regulated at the transcriptional level by ARE, breaks down heme into free iron, carbon monoxide iron and biliverdin. Because biliverdin is further degraded to bilirubin, which has strong antioxidant properties, HO-1 plays a potentially important role in antioxidant defense and iron homeostasis [54, 55]. These observations suggest that the application of antioxidants capable of activating the Nrf2/HO-1 signaling pathway could be adopted as a promising therapeutic strategy for the prevention and treatment of oxidative stress-mediated damage. In addition, various indole derivatives have been reported to have antioxidant properties that are mediated by the activation of the Nrf2/HO-1 signaling pathway to protect against the apoptosis caused by oxidative injury [27, 28, 30]. Based on these findings, we investigated whether the activation of the Nrf2/HO-1 signaling pathway was involved in the antioxidant efficacy of I6CA, and we found that I6CA *remarkably* increased the expression of the phosphorylated Nrf2 protein in the presence of H_2O_2. In addition, the expression of HO-1 and its activity increased under the same conditions, and Keap1 expression was downregulated, indicating that Nrf2 was activated in the I6CA-treated V79-4 cells under oxidative conditions. Therefore, we used ZnPP, a HO-1 inhibitor, to further elucidate the role of the Nrf2/HO-1 signaling pathway in the antioxidant effects of I6CA and found that the ROS scavenging ability of I6CA was eliminated by the presence of ZnPP. Concomitant with these results, the ZnPP significantly reversed the I6CA-mediated reduction in apoptosis in the presence of H_2O_2 and returned the levels of apoptosis to the levels observed in cells treated with H_2O_2 alone. These results demonstrate that the activation of the Nrf2/HO-1 signaling pathway may act as an upstream signal of the protective potential of I6CA against oxidative stress-induced V79-4 cell apoptosis.

Conclusion

In summary, in this study, we evaluated the protective effect of I6CA against H_2O_2-induced oxidative stress in V79-4 lung fibroblasts. According to our results, I6CA reversed the increased intracellular ROS production and mitochondrial damage caused by H_2O_2, eventually inhibiting DNA damage, cell cycle arrest at the G2/M phase and apoptosis. I6CA also activated Nrf2 and promoted the expression of its downstream target protein HO-1, which may have contributed to alleviating oxidative stress and improving oxidant resistance. Although this is the first study to demonstrate that I6CA can relieve H_2O_2-induced oxidative stress in lung fibroblasts by enhancing antioxidant capacity through activation of the Nrf2/HO-1 signaling pathway, further studies are required to assess how I6CA can regulate the transcriptional activity of Nrf2 and whether other signaling pathways can participate in the antioxidant activity of I6CA.

Acknowledgements

Author Contributions

Sung Ok Kim and Yung Hyun Choi designed the study; Sung Ok Kim performed the experiments; Sung Ok Kim wrote the original manuscript;, Yung Hyun Choi reviewed and edited the manuscript.

Funding

This work was supported by Basic Science Research Program through the National Research Foundation of Korea (NRF) grant funded by the Korea government (2018R1A2B2005705).

Statement of Ethics

The authors have no ethical conflicts to disclose.

Disclosure Statement

The authors have no conflicts of interest to declare.

References

1 Lv M, Liu Y, Ma S, Yu Z: Current advances in idiopathic pulmonary fibrosis: the pathogenesis, therapeutic strategies and candidate molecules. Future Med Chem 2019;11:2595-2620.
2 Chanda D, Otoupalova E, Smith SR, Volckaert T, De Langhe SP, Thannickal VJ: Developmental pathways in the pathogenesis of lung fibrosis. Mol Aspects Med 2019;65:56-69.
3 Cheng Z, Ristow M: Mitochondria and metabolic homeostasis. Antioxid Redox Signal 2013;19:240-242.
4 Kalyanaraman B, Cheng G, Hardy M, Ouari O, Bennett B, Zielonka J: Teaching the basics of reactive oxygen species and their relevance to cancer biology: Mitochondrial reactive oxygen species detection, redox signaling, and targeted therapies. Redox Biol 2018;15:347-362.
5 Osawa T: Development and application of oxidative stress biomarkers. Biosci Biotechnol Biochem 2018;82:564-572.
6 Roy J, Galano JM, Durand T, Le Guennec JY, Lee JC: Physiological role of reactive oxygen species as promoters of natural defenses. FASEB J 2017;31:3729-3745.
7 Larson-Casey JL, He C, Carter AB: Mitochondrial quality control in pulmonary fibrosis. Redox Biol 2020:8:101426.
8 Ballester B, Milara J, Cortijo J: Idiopathic pulmonary fibrosis and lung cancer: Mechanisms and molecular targets. Int J Mol Sci 2019;20:E593.

9 Prieto MA, López CJ, Simal-Gandara J: Glucosinolates: Molecular structure, breakdown, genetic, bioavailability, properties and healthy and adverse effects. Adv Food Nutr Res 2019;90:305-350.
10 Sánchez-Pujante PJ, Borja-Martínez M, Pedreño MÁ, Almagro L: Biosynthesis and bioactivity of glucosinolates and their production in plant *in vitro* cultures. Planta 2017;246:19-32.
11 Caruso A, Ceramella J, Iacopetta D, Saturnino C, Mauro MV, Bruno R, Aquaro S, Sinicropi MS: Carbazole derivatives as antiviral agents: An overview. Molecules 2019;24:1912.
12 Zhang MZ, Chen Q, Yang GF: A review on recent developments of indole-containing antiviral agents. Eur J Med Chem 2015;89:421-441.
13 Kaur J, Utreja D, Ekta, Jain N, Sharma S: Recent developments in the synthesis and antimicrobial activity of indole and its drivatives. Curr Org Synth 2019;16:17-37.
14 Garg V, Maurya RK, Thanikachalam PV, Bansal G, Monga V: An insight into the medicinal perspective of synthetic analogs of indole: A review. Eur J Med Chem 2019;180:562-612.
15 Ampofo E, Schmitt BM, Menger MD, Laschke MW: Targeting the microcirculation by indole-3-carbinol and its main derivate 3,3',-diindolylmethane: Effects on angiogenesis, thrombosis and inflammation. Mini Rev Med Chem 2018;18:962-968.
16 Sugimoto S, Naganuma M, Kanai T: Indole compounds may be promising medicines for ulcerative colitis. J Gastroenterol 2016;51:853-861.
17 Wang N, Świtalska M, Wang L, Shaban E, Hossain MI, El Sayed IET, Wietrzyk J, Inokuchi T: Structural modifications of nature-inspired indoloquinolines: A mini review of their potential antiproliferative activity. Molecules 2019;24:E2121.
18 Wang SY, Shi XC, Laborda P: Indole-based melatonin analogues: Synthetic approaches and biological activity. Eur J Med Chem 2020;185:111847.
19 Hasan H, Ismail H, El-Orfali Y, Khawaja G: Therapeutic benefits of indole-3-carbinol in adjuvant-induced arthritis and its protective effect against methotrexate induced-hepatic toxicity. BMC Complement Altern Med 2018;18:337.
20 Wan Y, Li Y, Yan C, Yan M, Tang Z: Indole: A privileged scaffold for the design of anti-cancer agents. Eur J Med Chem 2019;183:111691.
21 Sidhu JS, Singla R, Mayank, Jaitak V: Indole derivatives as anticancer agents for breast cancer therapy: A review. Anticancer Agents Med Chem 2015;16:160-173.
22 Hendrikx T, Schnabl B: Indoles: metabolites produced by intestinal bacteria capable of controlling liver disease manifestation. J Intern Med 2019;286:32-40.
23 Konopelski P, Ufnal M: Indoles - Gut bacteria metabolites of tryptophan with pharmacotherapeutic potential. Curr Drug Metab 2018;19:883-890.
24 Zhang Y, Li M, Li X, Zhang T, Qin M, Ren L: Isoquinoline alkaloids and indole alkaloids attenuate aortic atherosclerosis in apolipoprotein E deficient mice: A systematic review and meta-analysis. Front Pharmacol 2018;9:602.
25 Wei PC, Lee-Chen GJ, Chen CM, Wu YR, Chen YJ, Lin JL, Lo YS, Yao CF, Chang KH: Neuroprotection of indole-derivative compound NC001-8 by the regulation of the NRF2 pathway in Parkinson›s disease cell models. Oxid Med Cell Longev 2019;2019:5074367.
26 Niino T, Tago K, Yasuda D, Takahashi K, Mashino T, Tamura H, Funakoshi-Tago M: A 5-hydroxyoxindole derivative attenuates LPS-induced inflammatory responses by activating the p38-Nrf2 signaling axis. Biochem Pharmacol 2018;155:182-197.
27 Mohamed AF, El-Yamany MF, El-Batrawy FA, Abdel-Aziz MT: JNJ7777120 ameliorates inflammatory and oxidative manifestations in a murine model of contact hypersensitivity *via* modulation of TLR and Nrf2 signaling. Inflammation 2018;41:378-389.
28 Hajra S, Basu A, Singha Roy S, Patra AR, Bhattacharya S: Attenuation of doxorubicin-induced cardiotoxicity and genotoxicity by an indole-based natural compound 3,3'-diindolylmethane (DIM) through activation of Nrf2/ARE signaling pathways and inhibiting apoptosis. Free Radic Res 2017;51:812-827.
29 Hajra S, Patra AR, Basu A, Bhattacharya S: Prevention of doxorubicin (DOX)-induced genotoxicity and cardiotoxicity: Effect of plant derived small molecule indole-3-carbinol (I3C) on oxidative stress and inflammation. Biomed Pharmacother 2018;101:228-243.

30 Kim D, Kim H, Kim K, Roh S: The protective effect of indole-3-acetic acid (IAA) on H_2O_2-damaged human dental pulp stem cells is mediated by the AKT pathway and involves increased expression of the transcription factor nuclear factor-erythroid 2-related factor 2 (Nrf2) and its downstream target heme hxygenase 1 (HO-1). Oxid Med Cell Longev 2017;2017:8639485.
31 Kang MC, Ding Y, Kim EA, Choi YK, de Araujo T, Heo SJ, Lee SH: Indole derivatives isolated from brown alga *Sargassum thunbergii* inhibit adipogenesis through AMPK activation in 3T3-L1 preadipocytes. Mar Drugs 2017;15:119.
32 Kim TH, Heo SJ, Ko SC, Park WS, Choi IW, Yi M, Jung WK: Indole-6-carboxaldehyde isolated from *Sargassum thunbergii* inhibits the expression and secretion of matrix metalloproteinase-9. Int J Mol Med 2019;44:1979-1987.
33 Kim JS, Cho IA, Kang KR, Lim H, Kim TH, Yu SK, Kim HJ, Lee SA, Moon SM, Chun HS, Kim CS, Kim DK: Reversine induces caspase-dependent apoptosis of human osteosarcoma cells through extrinsic and intrinsic apoptotic signaling pathways. Genes Genomics 2019;41:657-665.
34 Yoon HJ, Chay KO, Yang SY: Native low density lipoprotein increases the production of both nitric oxide and reactive oxygen species in the human umbilical vein endothelial cells. Genes Genomics 2019;41:373-379.
35 Aristizabal-Pachon AF, Castillo WO: Genotoxic evaluation of occupational exposure to antineoplastic drugs. Toxicol Res 2019;36:29-36.
36 Kim DY, Kim JH, Lee JC, Won MH, Yang SR, Kim HC, Wie MB: Zinc oxide nanoparticles exhibit both cyclooxygenase- and lipoxygenase-mediated apoptosis in human bone marrow-derived mesenchymal stem cells. Toxicol Res 2019;35:83-91.
37 Ding Y, Zhang Z, Yue Z, Ding L, Zhou Y, Huang Z, Huang H: Rosmarinic acid ameliorates H_2O_2-induced oxidative stress in L02 cells through MAPK and Nrf2 pathways. Rejuvenation Res 2019;22:289-298.
38 Kang KA, Lee KH, Chae S, Zhang R, Jung MS, Kim SY, Kim HS, Kim DH, Hyun JW: Cytoprotective effect of tectorigenin, a metabolite formed by transformation of tectoridin by intestinal microflora, on oxidative stress induced by hydrogen peroxide. Eur J Pharmacol 2005;519:16-23.
39 Liu H, Liu W, Zhou X, Long C, Kuang X, Hu J, Tang Y, Liu L, He J, Huang Z, Fan Y, Jin G, Zhang Q, Shen H: Protective effect of lutein on ARPE-19 cells upon H_2O_2-induced G2/M arrest. Mol Med Rep 2017;16:2069-2074.
40 Karimian A, Ahmadi Y, Yousefi B: Multiple functions of p21 in cell cycle, apoptosis and transcriptional regulation after DNA damage. DNA Repair (Amst) 2016;42:63-71.
41 Swanton C: Cell-cycle targeted therapies. Lancet Oncol 2004;5:27-36.
42 Kim SY, Jo HY, Kim MH, Cha YY, Choi SW, Shim JH, Kim TJ, Lee KY: H_2O_2-dependent hyperoxidation of peroxiredoxin 6 (Prdx6) plays a role in cellular toxicity via up-regulation of iPLA2 activity. J Biol Chem 2008;283:33563-33568.
43 Seomun Y, Kim JT, Kim HS, Park JY, Joo CK: Induction of p21Cip1-mediated G2/M arrest in H_2O_2-treated lens epithelial cells. Mol Vis 2005;11:764-774.
44 Pei XH, Xiong Y: Biochemical and cellular mechanisms of mammalian CDK inhibitors: a few unresolved issues. Oncogene 2005;24:2787-2795.
45 Dutto I, Tillhon M, Cazzalini O, Stivala LA, Prosperi E: Biology of the cell cycle inhibitor p21(CDKN1A): molecular mechanisms and relevance in chemical toxicology. Arch Toxicol 2015;89:155-178.
46 Bock FJ, Tait SWG: Mitochondria as multifaceted regulators of cell death. Nat Rev Mol Cell Biol 2020;21:85-100.
47 Popgeorgiev N, Jabbour L, Gillet G: Subcellular localization and dynamics of the Bcl-2 family of proteins. Front Cell Dev Biol 2018;6:13.
48 Xiong S, Mu T, Wang G, Jiang X: Mitochondria-mediated apoptosis in mammals. Protein Cell 2014;5:737-749.
49 Er E, Oliver L, Cartron PF, Juin P, Manon S, Vallette FM: Mitochondria as the target of the pro-apoptotic protein Bax. Biochim Biophys Acta 2006;1757:1301-1311.
50 Kiraz Y, Adan A, Kartal Yandim M, Baran Y: Major apoptotic mechanisms and genes involved in apoptosis. Tumour Biol 2016;37:8471-8486.
51 Hassan M, Watari H, AbuAlmaaty A, Ohba Y, Sakuragi N: Apoptosis and molecular targeting therapy in cancer. Biomed Res Int 2014;2014:150845.
52 Shaw P, Chattopadhyay A: Nrf2-ARE signaling in cellular protection: Mechanism of action and the regulatory mechanisms. J Cell Physiol 2020;235:3119-3130.

53 Fetoni AR, Paciello F, Rolesi R, Paludetti G, Troiani D: Targeting dysregulation of redox homeostasis in noise-induced hearing loss: Oxidative stress and ROS signaling. Free Radic Biol Med 2019;135:46-59.
54 Yu ZY, Ma D, He ZC, Liu P, Huang J, Fang Q, Zhao JY, Wang JS: Heme oxygenase-1 protects bone marrow mesenchymal stem cells from iron overload through decreasing reactive oxygen species and promoting IL-10 generation. Exp Cell Res 2018;362:28-42.
55 Bonelli M, Savitskaya A, Steiner CW, Rath E, Bilban M, Wagner O, Bach FH, Smolen JS, Scheinecker C: Heme oxygenase-1 end-products carbon monoxide and biliverdin ameliorate murine collagen induced arthritis. Clin Exp Rheumatol 2012;30:73-78.